Partition energy absorption of axially crushed aluminum foam-filled hat sections

Hong-Wei Song [a,b,*], Zi-Jie Fan [b], Gang Yu [a], Qing-Chun Wang [b], A. Tobota [c]

[a] *Institute of Mechanics, Chinese Academy of Sciences, Beijing 100080, PR China*
[b] *State Key Laboratory of Automotive Safety and Energy, Department of Automotive Engineering, Tsinghua University, Beijing 100084, PR China*
[c] *Institute of Production Engineering and Automation, Mechanical Engineering Faculty, Wrocław University of Technology, Poland*

Abstract

The "interaction effect" between aluminum foam and metal column that takes place when foam-filled hat sections (top-hats and double-hats) are axially crushed was investigated in this paper. Based on experimental examination, numerical simulation and analytical models, a systemic approach was developed to partition the energy absorption quantitatively into the foam filler component and the hat section component, and the relative contribution of each component to the overall interaction effect was therefore evaluated. Careful observation of the collapse profile found that the crushed foam filler could be further divided into two main energy-dissipation regions: densified region and extremely densified region. The volume reduction and volumetric strain of each region were empirically estimated. An analytical model pertinent to the collapse profile was thereafter proposed to find the more precise relationship between the volume reduction and volumetric strain of the foam filler. Combined the superfolding element model for hat sections with the current model according to the coupled method, each component energy absorption was subsequently derived, and the influence of some controlling factors was discussed. According to the finite element analysis and the theoretical modeling, when filled with foam, energy absorption was found to be increased both in the hat section and the foam filler, whereas the latter contributes predominantly to the interaction effect. The formation of the extremely densified region in the foam filler accounts for this effect.
© 2004 Elsevier Ltd. All rights reserved.

Keywords: Aluminum foam; Thin-walled column; Interaction effect; Energy absorption; Axially compression

---

* Corresponding author. Address: Institute of Mechanics, Chinese Academy of Sciences, Beijing 100080, PR China. Tel.: +86 010 62651165; fax: +86 010 62521859.
  E-mail address: songhw@tsinghua.edu.cn (H.-W. Song).

1. Introduction

Weight-saving and impact safety requirements are calling for the application of light-weight materials and structures with high specific energy absorption to vehicles. Recently, much attention is given to the cellular material filled thin-walled structures (Chen, 2001; Hanssen et al., 2002; Kim et al., 2002; Santosa and Wierzbicki, 1999; Seitzberger et al., 2000). The studies showed that the interaction between metal or polymeric cellular material fillers and the supporting structures produces some desirable crushing behaviors and energy absorption properties. Among many optional cellular fillers, e.g., sawdust, honeycomb, polyurethane foam and metal foams, closed cell aluminum foam is the one gives some ideal performance.

Hanssen et al. (1999, 2000a,b,c, 2001a,b) performed comprehensive experimental and numerical studies on the axially crushing of aluminum foam-filled thin-walled aluminum columns, and these studies have built solid foundation and rich database for further theoretical studies and practical applications. Aluminum is a very attractive ultralight material, but it has drawbacks of machining and tooling difficulty, especially lack of efficient jointing technique: an aluminum structure can hardly be spot-welded. Meanwhile, when using aluminum extrusions, which themselves maintain the integrity, Hanssen et al. (2000c, 2002) found that a typical failure mode for foam-filled structures is rupture or ductile failure of the extrusion skin, which may harm the energy absorption. Considering these limitations, we used mild steel sections as the supporting structures in the current study.

Significant increase in crushing force and energy absorption was found in the foam-filled structures, and this phenomenon is now known as the interaction effect. However, up to now little work has been carried out to quantitatively determine this effect.

Some researchers have given numerical simulations and empirical discussions. Santosa and Wierzbicki (1998) developed a formula for the crushing force of foam-filled structures by using numerical simulation results. They found that the foam-wall interaction strength was of the same order as the uniaxial compressive strength of the foam, and concluded that the additional strength of the foam-filled column could be approximated as twice of the axial strength of the foam filler. Hanssen et al. (1999) suggested an empirical relationship, where the resultant crushing force was divided into three additive components: the crushing force of the non-filled extrusion, the uniaxial resistance of foam and the interaction effect between foam and extrusion. The interaction component is a function of geometrical parameters and material properties of foam and extrusion. These numerical or empirical studies did provide important cognition to the interaction effect, and might be more convincing if paralleled with rigorous theoretical analysis. Meanwhile, an analytical model with closed-form solution is necessary to provide a thorough evaluation on the contribution of each component to the interaction effect.

Abramowicz and Wierzbicki (1988) developed a general method to predict the crushing characteristics of foam-filled columns and gave a specific solution for the column filled with polyurethane foam. Reddy and Wall (1988) also calculated the crushing behavior of foam-filled cylindrical tubes. The basic assumption of these theoretical predictions is: the contribution of the dissipated energy from the compressed foam is independent from the deformed geometry of the supporting column, but is the function of volumetric strain and volume reduction of the foam. As a result, the mean crushing force was calculated by a simple sum of empty column component and strengthened foam component. According to this method, to determine the interaction effect of a foam-filled column, one key step is to find the equivalent volumetric strain and the volume change of the foam filler.

In the present study, hat sections made of mild steel were adopted while examining the interaction effect of foam-filled thin-walled structures. Hat sections are very commonly used in various vehicles, e.g., the front rails are typical top-hat sections, and the door pillars are typical double-hat sections, and they are the main crashworthy members that might dissipate a large amount of impact energy during an accident event. Preliminary experiments showed that the mean crushing force of the empty hat sections is several time higher than that of aluminum foam column in the same dimension (cross-section and height). No

spot-weld failure or rupture of the skin was found in the foam-filled sections, indicating a perfect matching-up of the filler and the supporting structure.

The energy absorption in each components of the foam-filled hat section was first examined from numerical simulation through LS-DYNA, and a preliminary quantitative partition was reached. Careful observation of the morphology of the crushed foam fillers finds three characteristic regions, and an analytical model corresponding to this collapse profile was subsequently proposed to obtain the volume reduction and volumetric strain in each region of the foam-filler. Combined with the analytical model of empty hat sections given by White and Jones (1999b), the crushing force of each part, i.e., hat section and foam filler, densified region and extremely densified region, was partitioned. The contribution of each component to the interaction effect in the foam-filled sections was therefore discussed. This analytical work is instructive to understand the energy absorption mechanism of foam-filled structures, and might be helpful for crashworthy design of these structures.

2. Experimental study

2.1. Specimens

The geometries of top-hat and double-hat sections are shown in Fig. 1. The corresponding dimensions in the figures are listed in Table 1. The sections were made of mild steel FEE355 with mechanical properties of stress at 0.2% strain $\sigma_{0.2} = 380$ MPa and ultimate stress $\sigma_u = 430$ MPa.
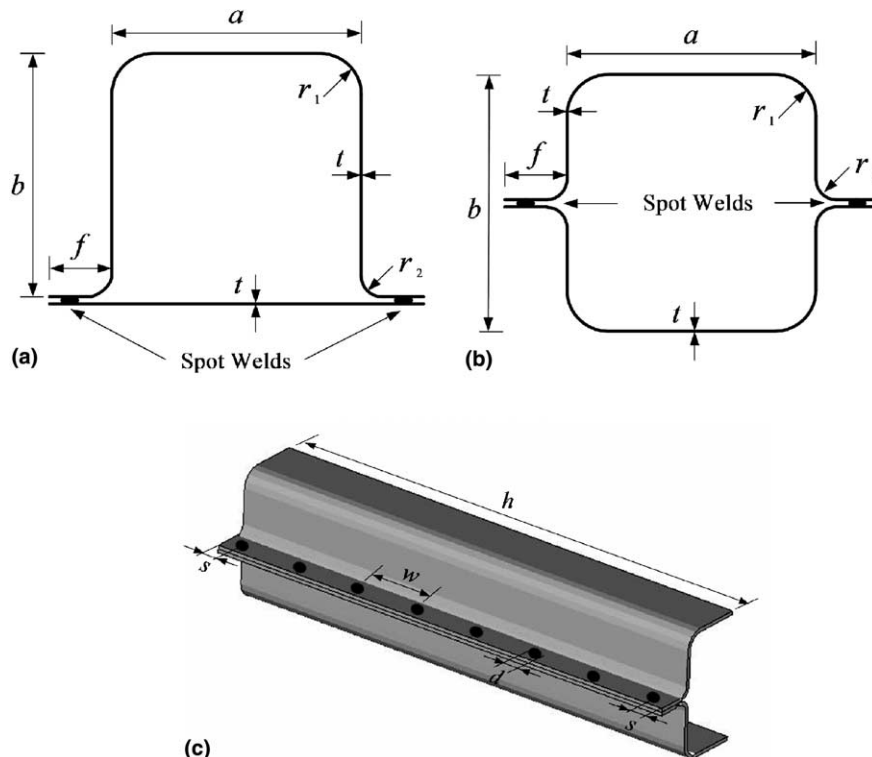

Fig. 1. Specimen geometry and spot-weld characters: (a) cross-section of a top-hat specimen; (b) cross-section of a double-hat specimen; (c) spot-weld arrangement, demonstrated in half of the double-hat.

Table 1
Geometry of hat sections

Wall thickness t (mm)	Width a (mm)	Width b (mm)	Height h (mm)	Flange f (mm)	Inner rolling radius r_1 (mm)	Outer rolling radius r_2 (mm)	Spot-weld spacing w (mm)	Edge spacing s (mm)	Spot-weld diameter d (mm)
1.5	50	50	200	15	6	4	27	5.5	6

It is noted that each type of the hat section is composed of two parts, therefore it has discontinuous walls. The top-hat comprises a hat with curved cross-section and a closing plate; and the double-hat comprises two hats with the same curved cross-section. The two parts were jointed by spot-weld, with the spot diameter of about $d = 6$ mm. Detailed spot-weld arrangement is also shown in Fig. 1 and listed in Table 1.

The closed-cell aluminum foam samples, named PML-725, were provided by Luoyang Material Research Institute of China. The aluminum foam was produced with the melt route technique, and the bulk products were cut into $50 \times 50 \times 200$ columns. Some of the aluminum foam columns were filled into the hat sections, others were left alone to perform fundamental tests (we call these specimens "free foam columns" in contrast with the "foam fillers"). Specific processing technique guaranteed the foam material could be produced in a relative stable density of about $\rho_f = 0.37$ g/cm^3 and the plateau stress σ_p of 4.82 MPa.

Non-filled hat sections, foam-filled hat sections and free aluminum foam columns were crushed axially under Instron 8506 testing machine at a constant cross-head speed of 5 mm/min, till 120 mm shortening was reached. To find the complete constitutive relationship, several free foam columns were crushed in a distance where the equivalent final strain reached 0.85.

2.2. Basic collapse modes

An axially crushed hat section tends to collapse in a stable manner. While filled with aluminum foam, the structure shows an even better stability. The basic collapse modes of the non-filled sections and their corresponding foam-filled sections are shown in Fig. 2. If crushed in a progressive manner, non-filled and foam-filled specimens share the similar collapse pattern, but the folding wavelength and the number of lobes may subject to change. In Fig. 2, when each specimen was crushed 120 mm in the axial direction, the non-filled hat sections formed 3 lobes, while the foam-filled sections formed as many as 5 lobes, for both top-hat and double-hat. As a result, the folding wavelength decreased in the filled sections. Another effect of foam filling is the decrease in the effective crushing distance, δ_{eff}. When measured from the collapsed specimens, δ_{eff} is about 0.75 times of folding wavelength in the empty sections, whereas it is 0.68–0.71 times of folding wavelength in the filled sections.

White and Jones (1999a) have summarized the collapse modes of top-hat and double-hat structures. The basic collapse modes observed in the current study are in accordance with those by White and Jones (1999a,b).
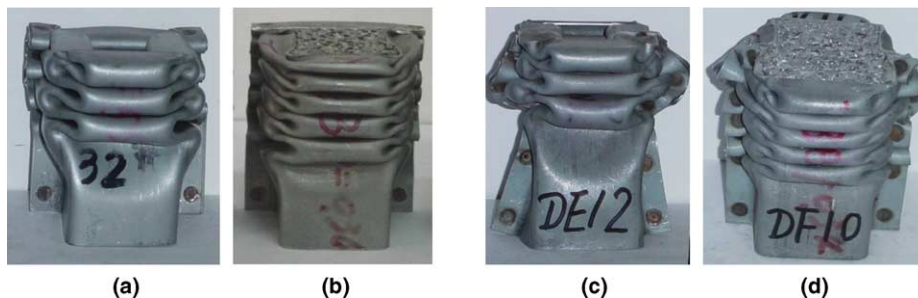

Fig. 2. Basic collapse modes: (a) empty top-hat; (b) foam-filled top-hat; (c) empty double-hat; (d) foam-filled double-hat.

2.3. Volume reduction and volumetric strain: experimental approximation

As stated in the introduction, volume change and volumetric strain of the foam filler need to be determined before the energy absorption and interaction effect could be evaluated.

To learn what was happened in the foam filler, some filled specimens were dissected by wire-cut technique through the middle plane along axial direction. A careful examination of the cut-away morphology of the crushed section shows that, the foam filler can be divided into three regions: (A) densified region; (B) extremely densified region; and (C) undeformed region, as shown in the enlarged photos in Fig. 3(a) (where the aluminum cells are in an inverse image) and the simplified diagrams in Fig. 3(b) and (c).

Aluminum foam can be taken as an ideal compressible material, whose lateral expansion could be neglected when uniaxially crushed. Therefore, the inner part of the foam filler could be approximated into a cubic, where it was subjected to the axial loading and was crushed in an equal cross-section manner. This part finally formed the "densified region". In the densified region, the foam cells were squeezed in the vertical direction and aligned in the horizontal direction, giving the clue of uniaxial crushing behavior. This character is illustrated in the enlarged morphology of foam cells in Fig. 3(a).
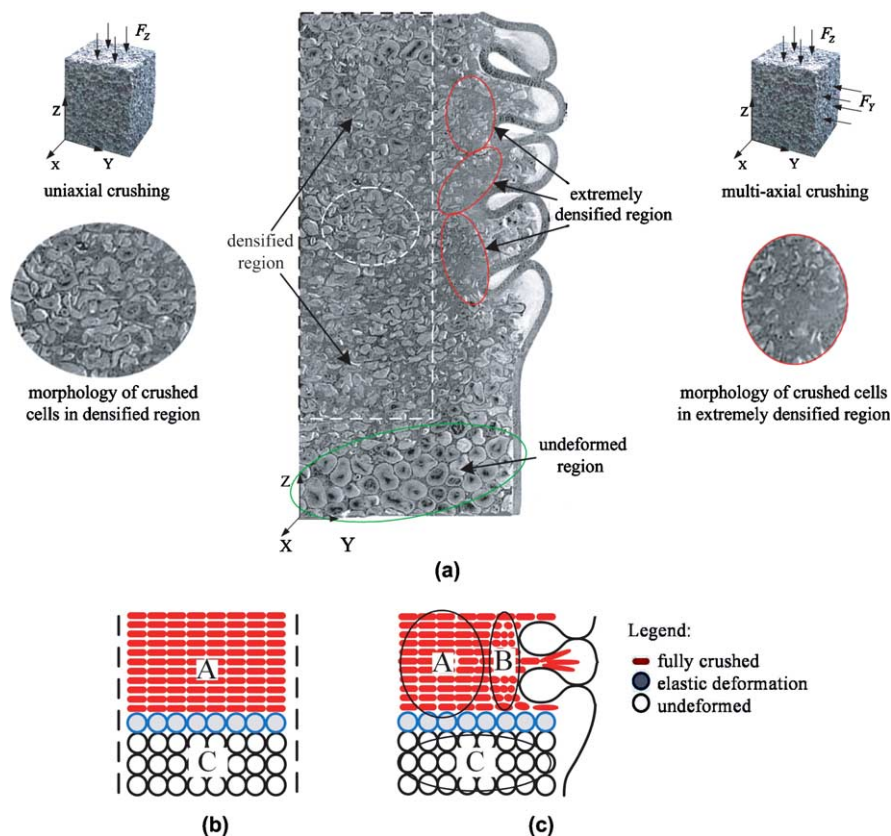

Fig. 3. Three characteristic regions in the crushed foam-filler. (a) Cut-away image of a crushed foam-filled hat section, on the left: uniaxial crushing and morphology of crushed cells, corresponding to the densified region; on the right: multi-axial crushing and morphology of crushed cells, corresponding to the extremely densified region. (b) and (c) are simplified diagrams of the inner part and surrounding part of the foam filler, where A denotes densified region, B denotes extremely densified region, C denotes undeformed region.

The surrounding part of the foam filler, however, shows a biaxial or multi-axial crushing characteristic. In this region, the foam cells were closely interacted with the sidewall of the supporting hat section as the folding waves processed. Under the combing actions of axial loading and inward folding of the sidewall, the foam cells were condensed till little room left. Unlike densified region, no obvious direction effect was found in this region. These characters can be inferred from the image of enlarged cells. Since the equivalent strain is extremely high, we name this region as the "extremely densified region".

In the region that is away from the crushing end, the foam cells maintained intact throughout the whole crushing process. This region is designated as the "undeformed region" since no deformation is observed if neglect the elastic effect. The existence of undeformed region reveals a progressive crushing characteristic of the aluminum foam material when filled.

To get an approximate volume change and volumetric strain of the foam filler, the undeformed region (region C in Fig. 3) should be accounted for first. Since there is no volume change in this region, the final strain can be written as

$$\varepsilon_{f3} = \frac{\Delta V_3}{V_{03}} = 0 \tag{1}$$

where ΔV_3 and V_{03} are the volume reduction and original volume in the undeformed region, respectively. Obviously $\Delta V_3 = 0$ indicates no contribution to the energy absorption in the undeformed region. This region is about 10 mm in length while measured from the collapsed specimens.

Secondly, consider the densified region (region A in Fig. 3). This region is a cubic with a constant crushing area in the cross-section. In the quasi-static experiments, the specimens with 200 mm in length were crushed in a distance of 120 mm. Suppose the cross-section of the cubic is a rectangle with the dimension of $m \times n$, remember the 10 mm undeformed region in length, the final strain of the densified region is

$$\varepsilon_{f1} = \frac{\Delta V_1}{V_{01}} = \frac{m \times n \times 120}{m \times n \times (200 - 10)} = 0.632 \tag{2}$$

where ΔV_1 and V_{01} are the volume reduction and original volume of the densified region, respectively.

Finally, consider the extremely densified region (region B in Fig. 3). Foam cells of this region subjected biaxial or multi-axial loading. Although both sidewall intrusion and foam cells extrusion exist, the intrusion effect is predominant, because the crushing strength of the mild steel is several times higher than that of the foam. The intrusion effect leads to an additional volume shrinkage in the direction perpendicular to the crushing. Consequently, the final strain of the extremely densified region is

$$\varepsilon_{f2} = \frac{\Delta V_2}{V_{02}} > 0.632 \tag{3}$$

where ΔV_2 and V_{02} are the volume reduction and original volume of the extremely densified region, respectively. The final volumetric strain in the representative deformed area therefore is

$$\bar{\varepsilon}_f = \frac{\Delta V_1 + \Delta V_2}{V_{01} + V_{02}} > 0.632 \tag{4}$$

The above experimental estimation gives a rough range for the final strain of the foam filler.

2.4. Interaction effect

Hanssen et al. (2000c) described the interaction effect as the following: the increased number of lobes created by introducing foam filler causes the force level of the foam-filled columns to be significantly higher than that of the combined effect of non-filled column and foam alone.

Similarly, the interaction effect is prominent in the foam-filled hat sections in the present study. Fig. 4 illustrated the interaction effect in the form of crushing force histories. And not only the crushing force,
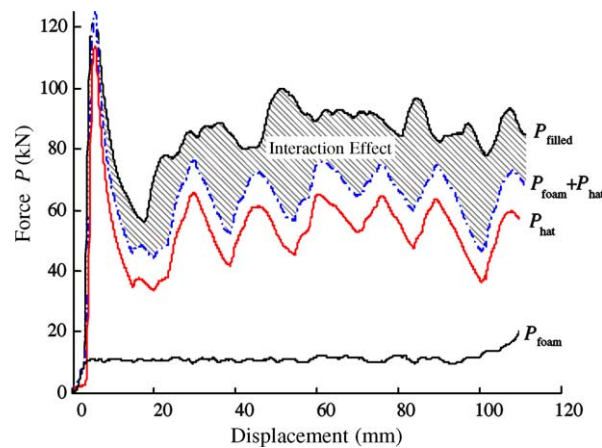
Fig. 4. The interaction effect of foam-filled hat section.

but also the specific energy absorption (energy absorbed per unit weight) of a foam-filled column shows the interaction effect. In Fig. 4, the shaded area is the increase in energy absorption due to the interaction effect. The interaction effect can be expressed in the following succinct diagram:

where each component can represent the corresponding crushing force or specific energy absorption. Also it can be written in the formula

$$P_{\text{filled}} > P_{\text{hat}} + P_{\text{foam}}$$
$$E_{\text{s,filled}} > E_{\text{s,hat}} + E_{\text{s,foam}}$$

(5)

where P stands for crushing force, E_{s} stands for specific energy absorption, subscription "fill", "hat" and "foam" stands for the filled hat section, empty hat section and free aluminum foam column, respectively. Two questions are therefore raised:

(1) The contribution of the thin-walled structure and the foam-filler to the total energy absorption?
(2) The relative contribution of the thin-walled structure and the foam-filler to the interaction effect?

It seems to be, however, a very tough task to quantitatively determine these two questions if merely from experiments. Numerical analysis and equivalent models are therefore adopted in the next steps to partition the energy absorption and evaluate the mechanism of interaction effect.

3. Numerical simulation

3.1. Finite element modeling

Numerical simulation using finite element codes is currently an important approach to learn in the crushing behaviors of foam-filled columns. Santosa et al. (2000), Hanssen et al. (2002) and Reyes et al. (2004), to

name some of the most recent work, used explicit dynamic finite element codes like LS-DYNA and PAM CRASH to perform this kind of simulation. Some key issues in the modeling, such as material model for aluminum foam, contact definition, friction effect, boundary condition and the bridge from dynamic to quasi-static were discussed.

In this work, nonlinear finite element LS-DYNA package was employed to simulate the crushing characteristics of foam-filled hat section. The sidewall of hat section was modeled with Belytschko-Tsay 4-node shell element, and the mild steel was modeled with plastic-kinematic material. The foam filler was modeled with 8-node solid element. The model is highly dependent upon the mesh quality and mesh size, due to the conditional stability characteristic for an explicit FE code. Shell elements and solid elements were modeled in a character size of 3.5 mm and 4 mm, respectively.

The difficulty is how to model the aluminum foam. Hanssen et al. (2002) gave an exhaustive study on validation of different available foam models in LS-DYNA, and concluded that none of the models managed to represent all load configurations with convincing accuracy. Therefore, one must prepared to neglect some trivial details and focus on the fundamentals while modeling. After careful validation, material model 63, i.e., crushable foam material in LS-DYNA (Hallquist, 1998) was selected to model the aluminum foam in the present study. The model assumes a constant Young's modulus, and the stress is updated by assuming an elastic behavior in the implementation. Strain–stress curve of the foam obtained from the uniaxial compression experiment was input into the model. Since the aluminum foam filler would undergo extremely high local compression and distortion, internal contact algorithm must be applied to the solid elements to prevent negative volume and numerical collapse. The interaction of the foam filler and column sidewall was simulated with automatic surface-to-surface contact.

Spot-weld is another controlling factor that affects the model quality. In the analysis, a spot-weld was modeled with 8 shell elements, which were defined in the same degrees of freedom. Rigid body property was assigned to the shell elements, because no fracture or failure or deformation was observed in the spot-weld in the experiments. Only half of the specimen was modeled due to the symmetry character. The load was applied at the upper end of the specimen with a constant displacement condition, through a rigid body which is modeled with shell elements.

3.2. Validation and verification

Validation and verification of the FE model is necessary before an effective partition work could be carried out. The material model for the aluminum foam was validated by the corresponding material test. The model of empty hat section was validated to examine the spot-weld modeling, mesh quality, and loading condition, etc. The validation work was also carried out on the model of foam-filled column to check if it could maintain calculation stability while undergoing very high local deformation and distortion in the filler, and check contact conditions as well.

Collapse mode and force history depict a complete crushing process, therefore, both the simulated collapse mode and force–displacement history need to be verified with the experiments. Figs. 5 and 6 give the verification of these two main aspects.

In Fig. 5, the simulated collapse modes are compared with those from experiments. For both empty and foam-filled columns, the simulated and actual collapse modes are very much alike, even in some detailed information, such as the folding wavelength, the number of lobes, and the effective crushing distance.

The comparison of simulated crushing force histories with the experiments also gives good agreement, for each result of empty top-hat, empty double-hat, foam-filled top-hat and foam-filled double-hat, as depicted in Fig. 6. The simulated mean crushing force is about 10% higher than that measured from corresponding experiment, because the loading rate in the model was increased to reduce the solution time for a quasi-static problem. In nonlinear dynamic FE codes like LS-DYNA and PAM-CRASH, explicit solution procedure is adopted to deal with impact problems in which inertia plays a dominant role. In order
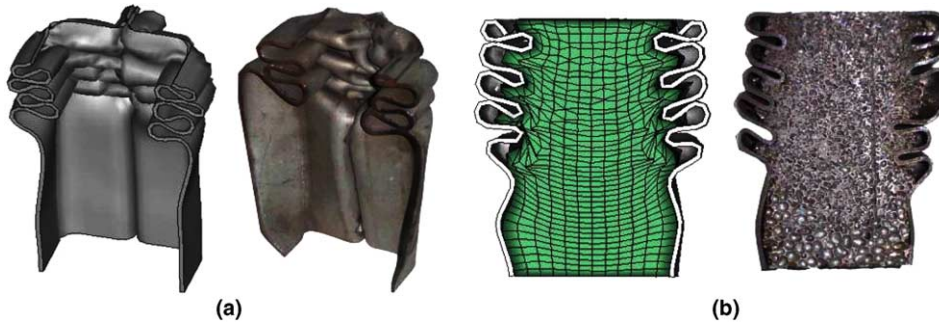
Fig. 5. Verification of collapse modes: (a) empty hat section, with the simulated on the left and experimental on the right; (b) foam filled hat section, with the simulated on the left and experimental on the right.
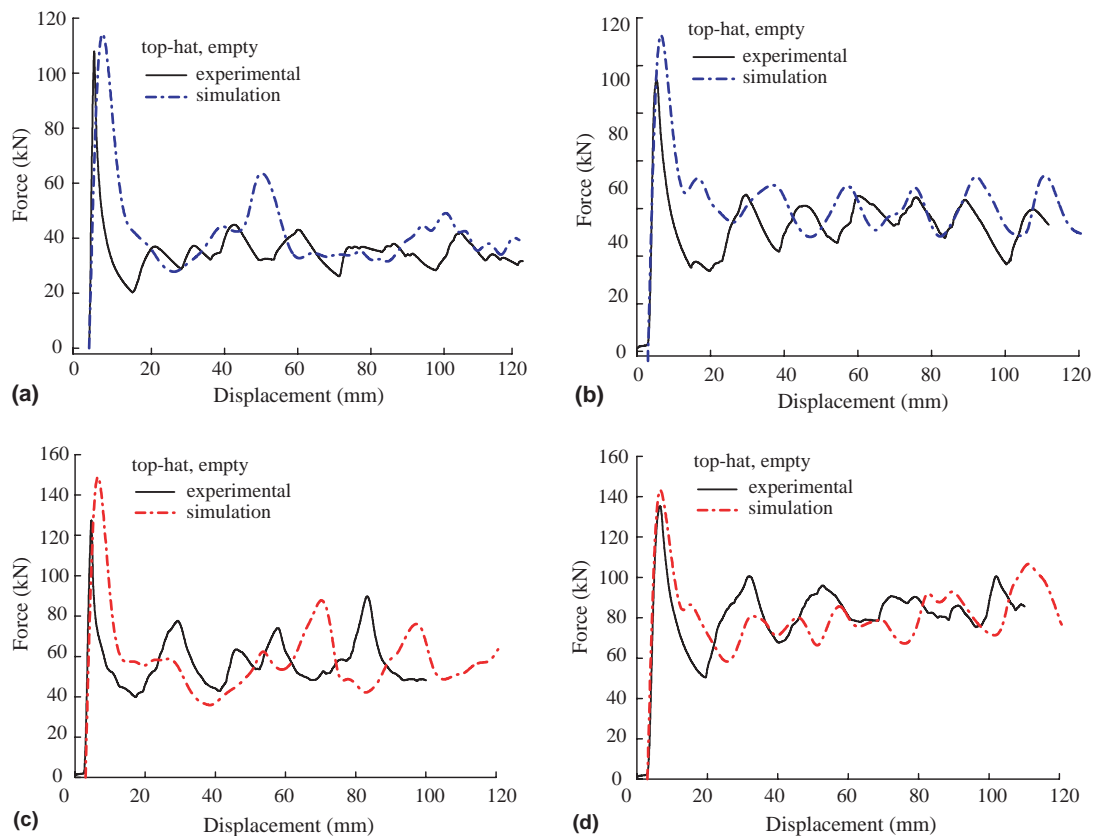

Fig. 6. Verification of crushing force histories: (a) empty top-hat; (b) empty double-hat; (c) filled top-hat; (d) filled double-hat.

to be compatible with the explicit solution, the load rate need to be accelerated to avoid large number of time step when modeling a quasi-static problem. Santosa et al. (2000) discussed how to bridge the gap from explicit dynamic procedure to quasi-static analysis.

3.3. Partition energy absorption and interaction effect via FE analysis

The advantage of numerical simulation over experiment is that the mechanical information of any desired part can be effectively obtained when the model is properly designed. By defining the right contact and part assembly relationships, the crushing histories of each component in the foam-filled structure, i.e., foam-filler component and supporting hat component, are separated, and so are the mean crushing forces and energy absorptions. Therefore, question (1) in Section 2.4 has been answered numerically. Meanwhile, individual empty hat sections and free foam columns are simulated under the same loading condition. The difference in the mean crushing force between the foam-filled structure and the sum of empty structure and free foam column is a quantitative expression of the so-called interaction effect. The interaction effect can be further divided into the relative contribution of the foam-filler and the supporting hat, by comparing the filler component with the free foam column, and comparing the hat section component with the empty hat section, respectively. Question (2) in Section 2.4 are therefore answered through numerical simulations.

Figs. 7–10 give the partition of both top-hat and double-hat in the form of force–displacement history, mean crushing force and collapse mode. These figures give the illustration of interaction effect and show how the energy absorption was distributed in each component of the filled column.
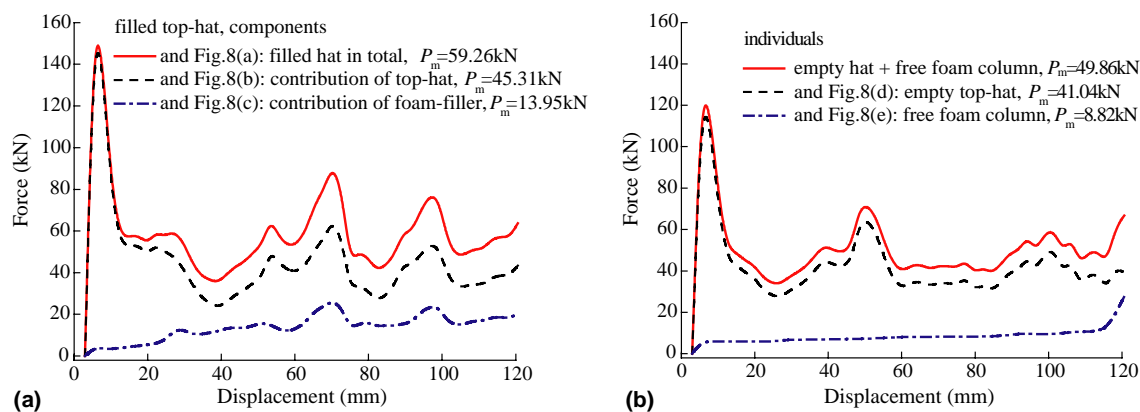

Fig. 7. Partition crushing force history of filled top-hat, and compared with corresponding individuals, simulation results: (a) foam-filed components; (b) corresponding individuals.
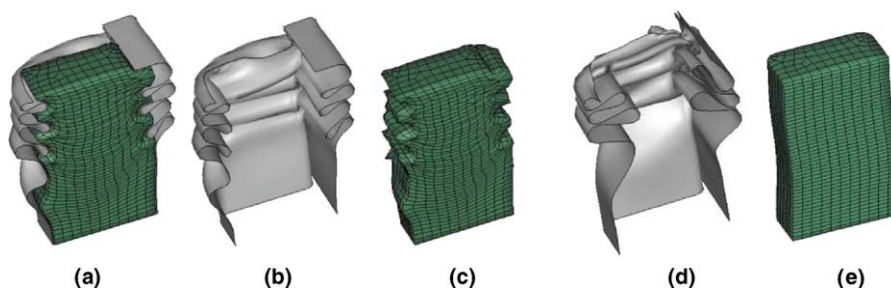

Fig. 8. Interaction effect expressed in the form of simulated collapse mode, when these modes represent the mean crushing force or energy absorption, one gets $(a) = (b) + (c)$; $(a) > (d) + (e)$ (a) foam-filled top-hat; (b) top-hat component; (c) foam-filler component; (d) empty top-hat; (e) free foam column.
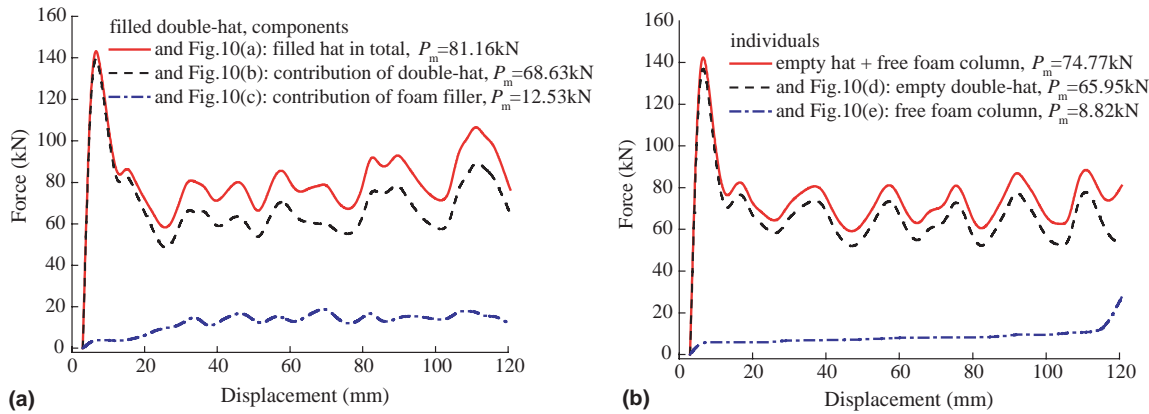
Fig. 9. Partition crushing force history of filled double-hat, and compared with corresponding individuals, simulation results. (a) foam-filled components; (b) corresponding individuals.
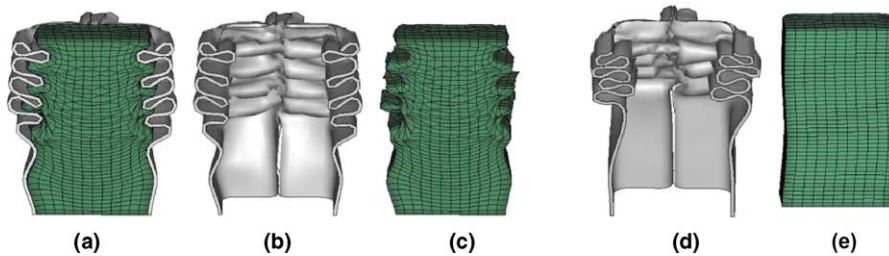

Fig. 10. Interaction effect expressed in the form of simulated collapse mode, when these modes represent the mean crushing force or energy absorption, one gets $(a) = (b) + (c)$; $(a) > (d) + (e)$: (a) foam-filled double-hat; (b) double-hat component; (c) foam-filler component; (d) empty double-hat; (e) free foam column.

The mean crushing force P_m of each component of the foam-filled section is listed in Table 2. Compared with its individual counterpart, P_m was found to be increased in both hat section and foam filler of the foam-filled section, and the contribution of each component to the interaction effect is therefore quantitatively measured.

Table 2
Partition energy absorption and contribution of interaction effect via FE analysis

Type		Hat section P_m (kN)	Foam P_m (kN)	Total P_m (kN)
Top-hat	Filled-hat components	45.31	13.95	59.26
	Individuals	41.04	8.82	49.86
	Increase in P_m	4.27	5.13	9.40
	(percentage increase)	(10.4%)	(58.1%)	(18.9%)
Double-hat	Filled-hat components	68.63	12.53	81.16
	Individuals	65.95	8.82	74.77
	Increase in P_m	2.68	3.71	6.39
	(percentage increase)	(4.1%)	(42.1%)	(8.5%)

Both foam filler and hat-section components show higher mean crushing force than their individual counterparts. It is demonstrated that the increase in energy absorption of the crushed foam-fillers compared to the free foam columns accounts for the main contribution to the interaction effect (with 58.1% and 42.1% increase in filled top-hat and double-hat, respectively). But due to the lower crushing strength of the foam, the total interaction effect of a filled column is about 18.9% and 8.5% increase in the mean crushing force, for top-hat and double-hat structures, respectively.

If the collapse modes in Figs. 8 and 10 stand for the mean crushing force or energy absorption of corresponding components and individuals, according to the results from Table 2 and also from Figs. 7 and 9, there exist

$$(a) = (b) + (c); \quad (b) > (d); \quad (c) > (e); \quad \text{and} \quad (a) > (d) + (e) \tag{6}$$

which is another vivid expression for the interaction effect.

4. Theoretical modeling

4.1. Outline of the general method

While examining the interaction effect of an axially compressed composite column like the foam-filled hat section, two general methods are applicable, which can be called "additive method" and "coupling method", respectively.

In the additive method, the mean crushing force of the composite column, $P_{m,f}$, may be divided into several additive components, which include the mean crushing force of each individual members when axially compressed, and the interaction effect

$$P_{m,f} = \sum P_{m,i} + P_{m,int} \tag{7}$$

where $P_{m,i}$ are the mean crushing forces of each individual members, which are obtained if the individual members (e.g., empty hat section, free foam column) are compressed axially, and $P_{m,int}$ is the contribution to $P_{m,f}$ resulting from the interaction effect. Obviously, in the additive method, the interaction effect is separated from each individual members.

Santosa and Wierzbicki (1998), Hanssen et al. (1999) and Seitzberger et al. (2000) used the additive method. For a square box column with a $b \times b$ cross-section, Santosa and Wierzbicki (1998) gave the prediction of the mean crushing force

$$P_{m,f} = P_{m,0} + 2b^2\sigma_f \tag{8}$$

where $P_{m,0}$ is the mean crushing force of empty column, σ_f is the crushing strength of the foam column. The contribution to $P_{m,f}$ from the interaction effect, which is in the same amount as the mean crushing force of foam column, equals $b^2\sigma_f$. While Hanssen et al. (1999) got an empirical expression

$$P_{m,f} = P_{m,0} + b^2\sigma_f + 5bt\sqrt{\sigma_f\sigma_0} \tag{9}$$

where t is the wall thickness, σ_0 is the flow stress of the structure material. The wall-foam strengthening interaction effect is a function of both material and geometrical parameters.

In the coupling method, however, the interaction effect is coupled in the mean crushing forces of each components, and the resultant mean crushing force of the composite member can be written as

$$P_{m,f} = \sum P_{m,i}^c \tag{10}$$

where $P_{\mathrm{m},i}^{\mathrm{c}}$ are the contributions to $P_{\mathrm{m,f}}$ from each component, and the strengthening interaction effects are coupled in $P_{\mathrm{m},i}^{\mathrm{c}}$. Taken foam-filled column as an example, the coupling method is obviously not a simple sum of contributions of empty column and foam column, because the mean crushing force of the thin-walled column may vary due to the changed folding wavelength and effective crushing distance, so may the foam filler. The changed folding wavelength can be obtained by minimum the energy absorption of the foam-filled column from the energy equilibrium. Basically, the procedure developed by Abramowicz and Wierzbicki (1988) predicting the mean crushing force of polyurethane foam-filled column is a coupling method.

In the current study, coupling method is adopted, because it can partition the energy absorption efficiently, as well as the interaction effect from each component.

4.2. Energy absorption model of non-filled hat sections

White and Jones (1999b) have given a theoretical analysis for the quasi-static axial crushing of top-hat and double-hat sections based on the superfolding elements (SE) method proposed and extended by Wierzbicki and Abramowicz (1983) and Abramowicz and Wierzbicki (1988, 1989). By simplifying the SE into "L" shape elements, White and Jones (1999b) gave the collapse profile of top-hat and double-hat structures with asymmetric elements, as shown in Fig. 11.

The analytical solution for a top-hat section gives the mean crushing force

$$P_{\mathrm{m}} = \frac{E_{\mathrm{top}}}{\delta_{\mathrm{eff}}} = M_0 \left\{ A_1 \frac{r}{t} + A_2 \frac{L}{H} + A_3 \frac{H}{r} \right\} \frac{2H}{\delta_{\mathrm{eff}}} \tag{11}$$

where E_{top} is the energy absorption of top-hat section when $2H$ sidewall is crushed, δ_{eff} is the effective crushing distance, $M_0 = \sigma_0 t^2/4$ is the fully plastic bending moment, t is the wall thickness of the hat section and σ_0 is the equivalent flow stress of the hat structure. $L = (2a + 2b + 4f)$ is the perimeter of the cross-section, r is the rolling radius for extensional elements in SE, H is the half wavelength of SE, coefficients $A_1 = 17.76$, $A_2 = \pi$, $A_3 = 9.184$. If discount the strain hardening of materials, Eq. (11) gives the final solution

$$\frac{P_{\mathrm{m}}}{M_0} = 32.89 \left(\frac{L}{t} \right)^{1/3} \tag{12}$$

$$\frac{H}{t} = 0.39 \left(\frac{L}{t} \right)^{2/3} \tag{13}$$
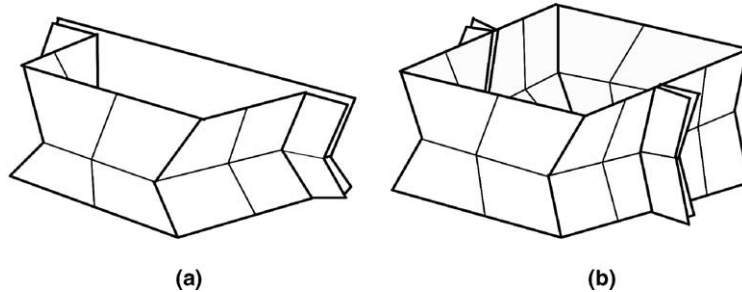

(a)   **(b)**

Fig. 11. Simplified crushing model for empty hat sections (White and Jones, 1999b): (a) top-hat section; (b) double-hat section.

Table 3
Comparison theoretical prediction (White and Jones, 1999b) with present experiments

Structure type	Item	Mean crushing force P_m (kN)	Half wavelength H (mm)	Error of P_m (%)	Error of H (%)
Top-hat	Experimental	36.2	23	12.7	20.4
	Theoretical	40.8	18.3		
Double-hat	Experimental	56.0	18	15.7	36.1
	Theoretical	64.8	11.5		

Similarly the crushing behavior of a double-hat section can be obtained

$$P_m = \frac{E_{\text{double}}}{\delta_{\text{eff}}} = M_0 \left\{ B_1 \frac{r}{t} + B_2 \frac{L}{H} + B_3 \frac{H}{r} \right\} \frac{2H}{\delta_{\text{eff}}} \tag{14}$$

where coefficients $B_1 = 35.52$, $B_2 = \pi$, $B_3 = 18.368$. And the solution gives

$$\frac{P_m}{M_0} = 52.20 \left(\frac{L}{t} \right)^{1/3} \tag{15}$$

$$\frac{H}{t} = 0.247 \left(\frac{L}{t} \right)^{2/3} \tag{16}$$

Since similar asymmetric collapse modes are found in the current study, we examined the above solution with the present experimental results. The geometrical parameters are: $L = 2a + 2b + 4f = 260$, and $t = 1.5$. It has been shown by Abramowicz and Wierzbicki (1989) that the energy equivalent flow stress σ_0 for progressively collapsing prismatic columns made of mild steel equals approximately to 0.92 times of the ultimate tensile strength σ_u. For the mild steel in the hat sections, $\sigma_u = 430$ MPa was measured from experiments, therefore, $\sigma_0 = 395.6$ MPa was used in the calculation. The comparison is listed in Table 3. The error of P_m is in an acceptable range of about 10%, whereas the theory seems to underestimate the half wavelength H by 20–36%.

4.3. Volume reduction and volumetric strain of foam filler: equivalent model

Similar approach proposed by Abramowicz and Wierzbicki (1988) was developed to determine the volume change and volumetric strain of aluminum foam fillers.

Aluminum foam can be treated as a perfectly compressible material, which is characterized by Poisson's ratio $\mu = 0$ in the plastic region. This means, when the foam column is uniaxially crushed, e.g., in the 1 directions, with the nominal stress σ_1 and nominal strain rate $\dot{\varepsilon}_1$, the other strain rate components $\dot{\varepsilon}_2$ and $\dot{\varepsilon}_3$ are equal to zero (Abramowicz and Wierzbicki, 1988). Therefore, the energy absorption rate of the foam column during uniaxial crushing can be written as

$$\dot{E}_{\text{foam}} = \int_{V_0} \sigma \dot{\varepsilon} \, dV = \int_{V_0} \sigma_1(V) \dot{V} \, dV \tag{17}$$

where V_0 is the initial volume of foam column. Suppose that Eq. (17) is valid for all combinations of principal strain rates $\dot{\varepsilon}_i$ ($i = 1, 2, 3$), the equivalent strain can be written in the function of volumetric relations

$$\varepsilon_f = 1 - \frac{V_{\text{final}}}{V_0} = \frac{\Delta V}{V_0} \tag{18}$$

where V_{final} and ΔV are the final volume and volume reduction, respectively. Integrating Eq. (17), one gets the energy absorption for uniform distribution of $\dot{V}$

$$E_{\text{foam}} = \bar{\sigma} \Delta V \tag{19}$$

Eqs. (18) and (19) show that when the volume change ΔV and the mean stress $\bar{\sigma}$ at a given final strain ε_f are obtained, the energy absorption of the foam structure can be subsequently calculated. Therefore, the main objective now turns to find the volumetric relationship and the constitutive relationship of the foam. And this is the reason why the important assumption could be made for a foam-filled column, i.e., the contribution of the dissipated energy from the crushed foam filler is independent from the deformed geometry of the column, and is merely a function of volumetric strain and volume reduction of itself.

Referring to the collapsed specimens and the cut-away images from different viewing points in Fig. 12, the interaction tendency between the foam filler and the hat-section could be revealed. Taking the filled top-hat as an example, each of the three viewing points from the profile shows intrusion effect of the section wall when the original foam column width was taken as the reference line. Whereas only A1–A2 section has some insignificant extrusion of aluminum foam, and no aluminum foam extrusion were observed in B1–B2 and C1–C2 sections, as can been seen in Fig. 12(a). The collapsed profiles of foam-filled double-hat sections show the similar tendency. This means, the inside folding effect of sidewalls is predominant, leading to a further volume shrinkage in the perimeter direction.

Based on the above observation, the deformation mode of foam filler can be modeled by neglecting some trivial or local irregularity in the actual crushed profile. Fig. 13 gives several possible modes, and these modes are equivalent in the volume aspects. Although its energy absorption is independent upon the specific collapse configuration according to the assumption, the foam filler should be modeled in a pertinent mode containing enough information that connects the crushing behavior of metal column. Therefore, a
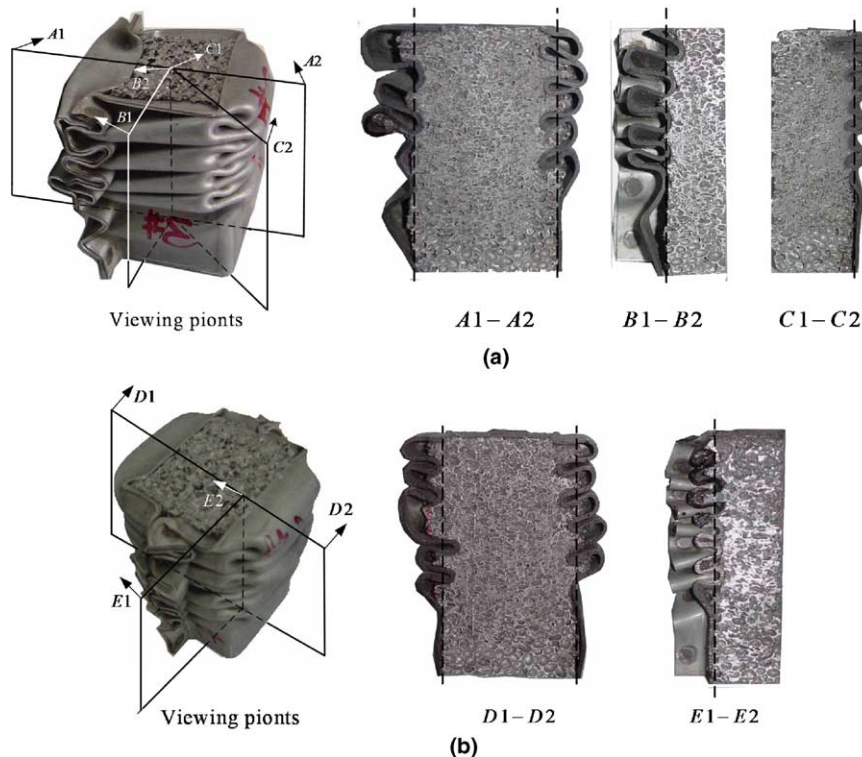

Fig. 12. Examining the collapsed profile due to the interaction of foam and hat structure from different viewing points: (a) top-hat section; (b) double-hat section.
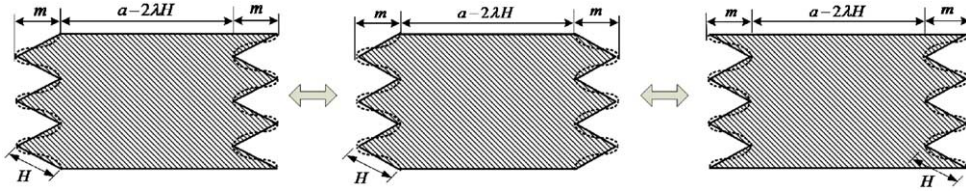
Fig. 13. Equivalent modes for the deformed foam filler, these modes are in the same final volume.

representative deformation model need to be selected, and this model should be simple yet sufficiently general to capture the main features of the crushing process.

Taking an original $2H$ length as the representative, suppose 3/4 of the final deformed fold is inside to the reference line, and the other 1/4 is outside to the reference line, the equivalent collapse model could be built to measure the volume reduction and volumetric strain of foam-fillers, as shown in Fig. 14. The model can be further divided into two parts: equal cross-section crushed region (or the densified region); and the surrounding region (or the extremely densified region).

The effective crushing distance of a foam-filled structure is

$$\delta_{\text{eff}} = 2\kappa H \tag{20}$$

where κ is the coefficient of effective crushing distance. Abramowicz and Wierzbicki have discussed the value of δ_{eff}, and found $\delta_{\text{eff}}/2H = 0.75$ for empty sheet metal columns (Abramowicz and Wierzbicki, 1989) and $\delta_{\text{eff}}/2H = 0.73$ for polyurethane foam-filled square columns (Abramowicz and Wierzbicki, 1988), respectively. According to the present experiments, κ is measured about 0.75 for the empty hat sections, whereas it is among 0.68–0.71 for the aluminum foam-filled hat sections. It seems that the effective crushing distance tends to decrease as the strength of the foam filler increases.

Setting $\lambda = \frac{3}{4}\sqrt{1-(1-\kappa)^2}$, the part that will be crushed into densified region (region ① in Fig. 14) is a cuboid with a constant cross-section of $(a - 2\lambda H)(b - 2\lambda H)$. Noteworthy that the final strain across this part is actually not the same, but it is much more uniform than the edge regions in which the foam was
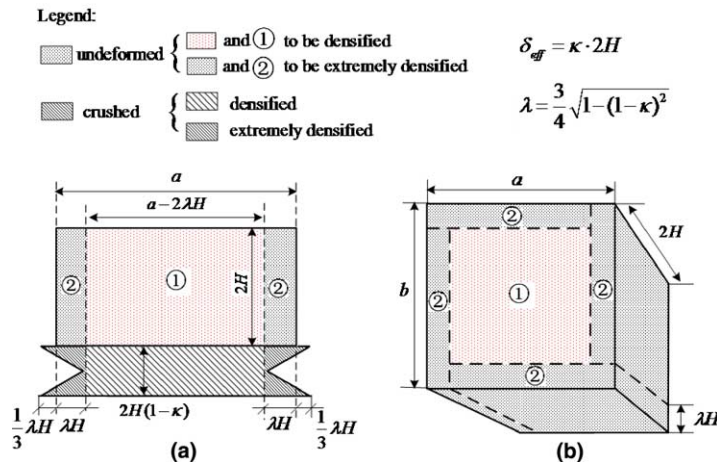

Fig. 14. Equivalent collapse model for determining the volume reduction and volumetric strain of the foam-filler: (a) side view, with one representative configuration before crush and one after crush; (b) bird view, before crush.

closely interacted with the deformed sidewalls of the hat section. The final volume V_{f1}, volume reduction ΔV_1 and volumetric final strain ε_{f1} of the densified region are

$$V_{f1} = (2H - \delta_{\text{eff}})(a - 2\lambda H)(b - 2\lambda H) = 2H(1 - \kappa)(a - 2\lambda H)^2 \tag{21}$$

$$\Delta V_1 = \delta_{\text{eff}}(a - 2\lambda H)(b - 2\lambda H) = 2\kappa H(a - 2\lambda H)^2 \tag{22}$$

$$\varepsilon_{f1} = \frac{\Delta V_1}{V_{01}} = \frac{\delta_{\text{eff}}(a - 2\lambda H)(b - 2\lambda H)}{2H(a - 2\lambda H)(b - 2\lambda H)} = \frac{\delta_{\text{eff}}}{2H} = \kappa \tag{23}$$

respectively. The surrounding parts, i.e., regions ② in Fig. 14(b), are closely interacted with the deformed walls and consequently form the extremely densified region. Setting the edges of the original (or undeformed) foam-filler as the reference lines, the extremely densified region comprises predominately intrusion of the sidewalls, which causes an additional reduction in the cross-sectional area and the extremely high volumetric strain. Referring to Fig. 14, the final volume V_{f2}, volume reduction ΔV_2 and volumetric final strain ε_{f2} of the extremely densified region are

$$V_{f2} = 4(1 - \kappa)H \cdot \sqrt{1 - (1 - \kappa)^2}H \cdot \left(a - \frac{3}{4}\sqrt{1 - (1 - \kappa)^2}H \right) = \frac{16}{3}H^2\lambda(1 - \kappa)(a - \lambda H) \tag{24}$$

$$\Delta V_2 = 8H^2\lambda(a - \lambda H) - \frac{16}{3}H^2\lambda(1 - \kappa)(a - \lambda H) = \frac{8}{3}H^2\lambda(1 + 2\kappa)(a - \lambda H) \tag{25}$$

$$\varepsilon_{f2} = \frac{\Delta V_2}{V_{02}} = \frac{\frac{8}{3}H^2\lambda(1 + 2\kappa)(a - \lambda H)}{8H^2\lambda(a - \lambda H)} = \frac{1 + 2\kappa}{3} \tag{26}$$

respectively. The total mean volumetric strain is

$$\bar{\varepsilon}_f = \frac{\Delta V_1 + \Delta V_2}{V} = \frac{3\kappa(a - 2\lambda H)^2 + 4H(1 + 2\kappa)(a - \lambda H)}{3a^2} \tag{27}$$

Since κ is among 0.68–0.71, the volumetric strain of densified region (or the equal cross-section crushed region) ε_{f1} is around 0.68–0.71, and the strain of the extremely densified region is around 0.79–0.81.

4.4. Partition energy absorption and interaction effect via analytical model

The above model shows that local strain in the crushed foam filler may exceed 0.8. To capture the overall crushing characteristic of the foam material, several free aluminum foam columns in the same dimension as that of the filler were compressed uniaxially till an extremely high final strain of over 0.85, and the typical history is shown in Fig. 15. According to the figure, the strain–stress history of an aluminum foam column can be divided into two stages: (1) a long stable crushing stage with a relative constant stress, which is denoted as the plateau stress σ_p; (2) a steep increase in stress after a specific strain, which is denoted as the densification strain ε_c. When fitted from the experimental curve, the constitutive relationship can be written in the function

$$\sigma(\varepsilon) = \begin{cases} \sigma_p, & \text{when } \varepsilon < \varepsilon_c \\ F(x)\sigma_p, & \text{when } \varepsilon > \varepsilon_c \end{cases} \tag{28}$$

The stress after ε_c can be fitted with various functions. The exponential function $F(x) = 1 + a_0 e^{x/b_0}$ ($x = \varepsilon$) demonstrates a more succinct expression and is very convenient in the current study, where parameters are $a_0 = 2.3 \times 10^{-5}$ and $b_0 = 0.06411$.
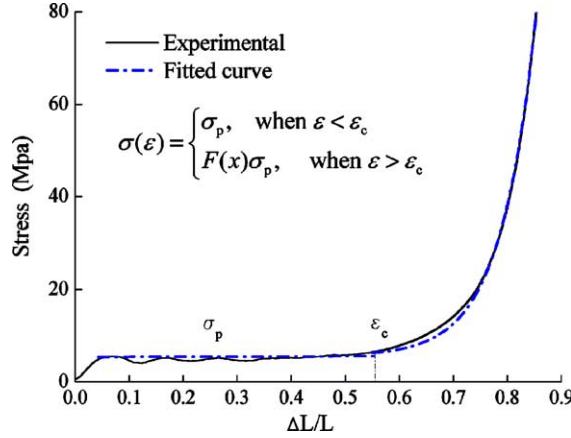
Fig. 15. Stress–strain relationship of aluminum foam.

The mean stress at a specific final strain ε_f is

$$\bar{\sigma}(\varepsilon_f) = \frac{1}{\varepsilon_f}\int_0^{\varepsilon_f}\sigma(\varepsilon)\,d\varepsilon = \frac{1}{\varepsilon_f}\left(\int_0^{\varepsilon_c}\sigma_p\,d\varepsilon + \int_{\varepsilon_c}^{\varepsilon_f}(1+a_0 e^{x/b_0})\sigma_p\,dx\right) = \sigma_p + \frac{1}{\varepsilon_f}a_0 b_0 \sigma_p(e^{\varepsilon_f/b_0} - e^{\varepsilon_c/b_0}) \quad (29)$$

Suppose $\kappa = 0.70$, which is a value normally measured from the experimental results, one gets the strain of densified region $\varepsilon_{f1} = 0.70$ and the strain of extremely densified region $\varepsilon_{f2} = 0.80$, from Eqs. (23) and (26), respectively. The densification strain of the aluminum foam is $\varepsilon_c = 0.55$, according to the experiment. Substituting strains in Eq. (29) by the above values, the mean stresses of densified region and extremely densified region are obtained

$$\begin{aligned}\bar{\sigma}(\varepsilon_{f1}) &= 1.1016\sigma_p\\ \bar{\sigma}(\varepsilon_{f2}) &= 1.4781\sigma_p\end{aligned} \quad (30)$$

When $2H$ sidewall is crushed, the energy absorption in the foam-filler is

$$\begin{aligned}E_{foam} &= \bar{\sigma}\Delta V = \bar{\sigma}(\varepsilon_{f1})\Delta V_1 + \bar{\sigma}(\varepsilon_{f2})\Delta V_2\\ &= \bar{\sigma}(\varepsilon_{f1})[2\kappa H(a-2\lambda H)^2] + \bar{\sigma}(\varepsilon_{f2})\left[\frac{8}{3}H^2\lambda(1+2\kappa)(a-\lambda H)\right]\end{aligned} \quad (31)$$

Substituting $\kappa = 0.70$ ($\delta_{eff} = 1.4H$) and Eq. (30) into Eq. (31), one gets

$$E_{foam} = \sigma_p[C_1(a-2\lambda H)^2 + C_2 H(a-\lambda H)]\cdot 2H \quad (32)$$

where the coefficients C_1 and C_2 are the function of geometrical and material parameters of the structure. Here $C_1 = 0.7711$ and $C_2 = 3.384$.

The next step, suppose the foam-filled hat sections collapse in the same modes the empty ones, i.e., the deformed modes of filled columns can still be simplified into those depicted in Fig. 11, whereas the wavelength and effective crushing distance may subject to change. The foam filler is assumed to deform together with the hat, while maintaining the volume change and energy absorption characters obtained from the above deduction. According to the coupling method, the total energy absorption of the foam-filled structures during $2H$ crushing is

$$E_{filled} = E_{hat} + E_{foam} \quad (33)$$

E_{hat} can be replaced by E_{top} and E_{double} in Eqs. (11) and (14). Therefore, the mean crushing forces of foam-filled top-hat and double hat structures are

$$\overline{P}_{s,filled} = \left\{ M_0 \left(A_1 \frac{r}{t} + A_2 \frac{L}{H} + A_3 \frac{H}{r} \right) + \sigma_p [C_1(a - 2\lambda H)^2 + C_2 H(a - \lambda H)] \right\} \frac{2H}{\delta_{eff}} \tag{34}$$

$$\overline{P}_{d,filled} = \left\{ M_0 \left(B_1 \frac{r}{t} + B_2 \frac{L}{H} + B_3 \frac{H}{r} \right) + \sigma_p [C_1(a - 2\lambda H)^2 + C_2 H(a - \lambda H)] \right\} \frac{2H}{\delta_{eff}} \tag{35}$$

respectively. The values of H and r should make the energy absorption reach the minimum, i.e.,

$$\frac{\partial \overline{P}_{filled}}{\partial H} = 0, \quad \frac{\partial \overline{P}_{filled}}{\partial r} = 0 \tag{36}$$

From $\frac{\partial \overline{P}_{filled}}{\partial r} = 0$ one gets $r = \sqrt{\frac{A_3 H t}{2A_1}}$, therefore

$$2\sigma_p \lambda (C_2 - 4C_1)H^3 - \sigma_p a(C_2 - 4\lambda C_1)H^2 - M_0 \sqrt{\frac{A_1 A_3 H^3}{t}} + M_0 A_2 L = 0 \tag{37}$$

Substituting geometrical parameters a, L and t; material parameters σ_0 and σ_p; coefficients A_1, A_2, A_3 (or B_1, B_2, B_3), C_1 and C_2 into Eq. (37), an expression comprising solely H is obtained. A computer code incorporated iterative algorithm is programmed to find the half wavelength H and the corresponding mean crushing loads, contributions due to hat structures and foam-filler, and contributions due to the densified region and extremely densified region, respectively.

4.5. Analytical results

The comparison of theoretical and experimental results, as well as the comparison of empty structures and filled structures can be found in Table 4. The model gives good prediction in term of mean crushing force, with an error of 6.0% and 2.2% for filled top-hat and double-hat, respectively. The comparison also shows a decrease in the half wavelength H when filled with aluminum foam, which is in agreement with the experimental observation.

Table 4
Comparison of theoretical and experimental results of foam-filled hat sections

Type	Item	Empty hat P_m (kN)	Filled hat P_m (kN)	Empty hat H (mm)	Filled hat H (mm)
Top-hat	Experimental	36.2	57.6	23	18
	Theoretical	40.8	61.08 (6.0% error)	18.3	14.51
Double-hat	Experimental	56.0	82.8	18	16
	Theoretical	64.8	84.6 (2.2% error)	11.5	10.32

Table 5
Partition energy absorption and contribution of interaction effect via theoretical prediction, in term of mean crushing force P_m

Type	Individuals			Foam-filled components			Contribution to the interaction effect		
	Empty hat (kN)	Free foam column (kN)	Sum (kN)	Hat section component (kN)	Foam filler component (kN)	Total (kN)	Increase in hat section kN/(%)	Increase in foam filler kN/(%)	Total increase kN/(%)
Top-hat	40.8	12.24	52.32	43.15	17.93	61.08	2.35/(5.8)	5.69/(46.5)	8.76/(16.7)
Double-hat	64.8	12.24	77.04	67.76	16.84	84.6	2.96/(4.6)	4.60/(37.6)	7.56/(9.8)

Energy absorption partition and contribution to the interaction effect from each component of foam-filled hat sections are listed in Table 5, according to the analytical model. To determine the mean crushing force of the free foam column, the mean stress is estimated by Eq. (29) and one obtains $\bar{\sigma}(0.6) = 1.0155\sigma_p$, then it is multiplied by the cross-sectional area of the column. The increase in the mean crushing force (contribution to the interaction effect) in the hat section component is 5.8% and 4.6% for the filled top-hat and double-hat, respectively, whereas the increase of P_m in the foam filler component is 46.5% and 37.6%, respectively. The analytical results further demonstrate that the aluminum foam filler contributed predominantly to the interaction effect.

From Eq. (37), the influence of plateau stress σ_p of foam material on H and P_m could be investigated. The increase of σ_p leads to a decrease of H and increase of P_m, see Fig. 16. Therefore, it seems to be an efficient way to augment energy absorption by applying a high strength foam material. However, this is under the assumption that the collapse mode is not seriously affected by the variation of σ_p. When $\sigma_p = 0$, the model reduces to the same result given by White and Jones (1999b).
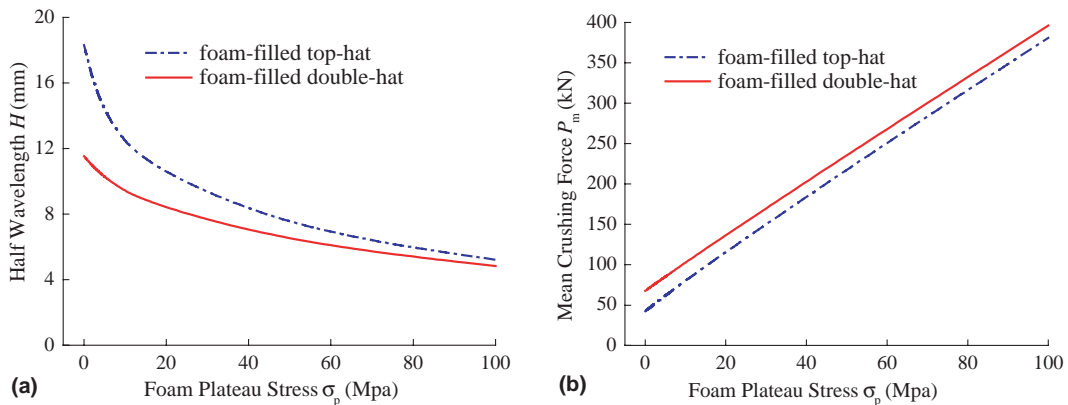

Fig. 16. Influence of foam plateau stress on H and P_m: (a) half wavelength H; (b) mean crushing force P_m.
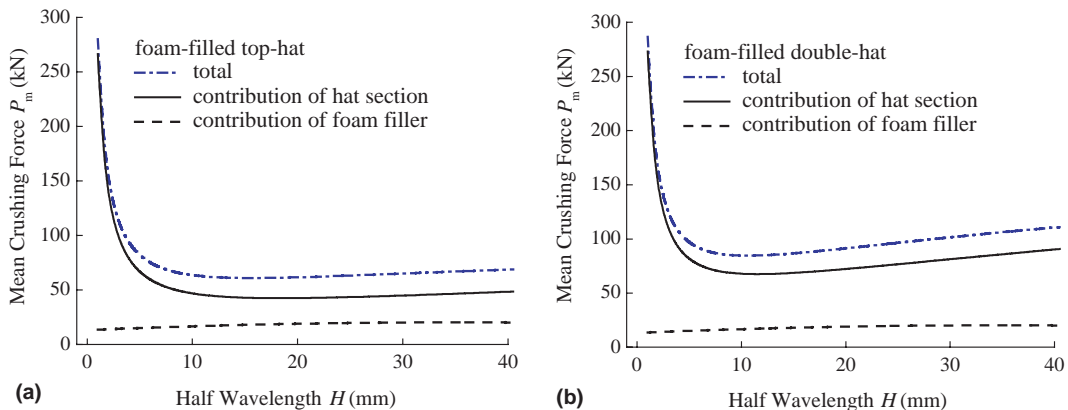

Fig. 17. Mean crushing force vs. H: (a) foam-filled top-hat; (b) foam-filled double-hat.

Similarly, one can get the influence of geometrical parameters (such as a, L and t) and material parameters (such as σ_0) to the half wavelength H and the mean crushing force P_m not listed here for space saving.

Fig. 17 examines the influence of H to P_m when geometrical parameters and material parameters do not subject to change. This is also the diagram showing how to obtain the optimum H. A pertinent value of H should make the mean crushing force of the foam-filled section reach the minimum, instead of the empty hat section. That is the reason why the H decreases significantly when filled with the foam.

The analytical model can efficiently partition the energy absorption of each component of the foam-filled hat section. Fig. 18 shows that when σ_p increases, the energy absorption of foam filler component augments significantly, whereas the hat component increases somewhat due to the reduced wavelength and increased folding number. Meanwhile, the energy absorption of densified region
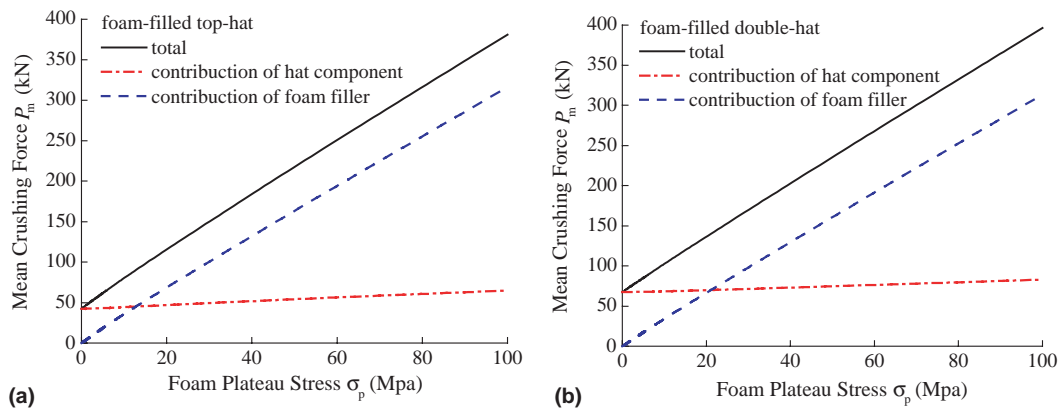

Fig. 18. Contributions of foam-filler and hat section to the mean crushing force of the foam-filled structure as a whole: (a) foam-filled top-hat; (b) foam-filled double-hat.
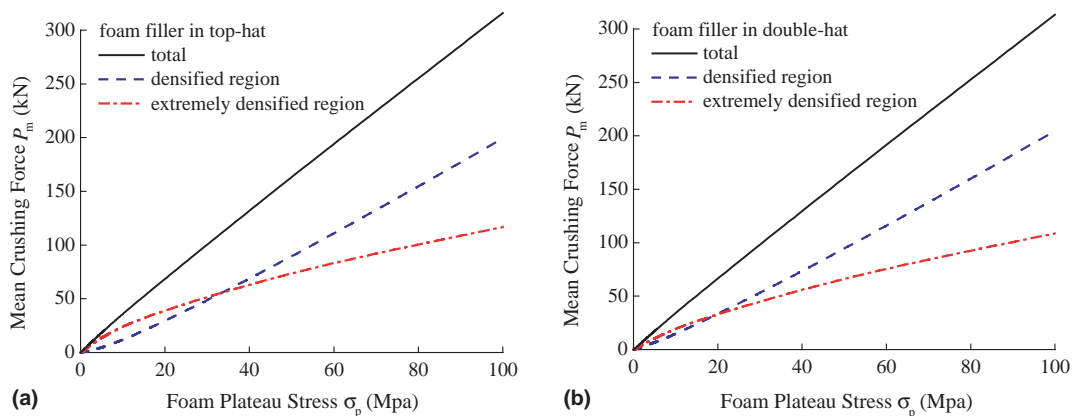

Fig. 19. Contributions of densified region and extremely densified region to the energy absorption: (a) foam-filled top-hat; (b) foam-filled double-hat.

and extremely densified region are partitioned. Fig. 19 shows that the contribution of the extremely den-sified region is dominant when σ_p is small (less than 33 MPa and 19 MPa for top-hat and double-hat, respectively), whereas the contribution of the densified region increases significantly as σ_p increases.

5. Discussions

5.1. Alternative simplified model

A simplified equivalent model for the foam filler was proposed to find if the basic assumption that energy absorption of foam filler is merely a function of volume change is applicable in the filled section. Also referring to Fig. 12, from the point of view of average and volume equivalence, we can assume the sidewalls of two opposite edges intrude by $H/2$ while there is no wall-intruding or foam extruding in the other 2 edges, or, more efficiently, assume each wall of the 4 edges intrudes by $H/4$ and there is no foam extruding, as depicted in Fig. 20.

Similar analysis can be processed. The final volume V_{f1}, volume reduction ΔV_1 and volumetric final strain ε_{f1} of the densified region are

$$V_{f1} = \frac{1}{4}(2H - \delta_{eff})(2a - H)^2 \tag{38}$$

$$\Delta V_1 = \frac{1}{4}\delta_{eff}(2a - H)^2 \tag{39}$$

$$\varepsilon_{f1} = \frac{\Delta V_1}{V_{01}} = \frac{\delta_{eff}}{2H} = \kappa \tag{40}$$

respectively. V_{f2}, ΔV_2 and ε_{f2} of the extremely densified region are

$$V_{f2} = \frac{1}{8}H(2H - \delta_{eff})(4a - H) \tag{41}$$

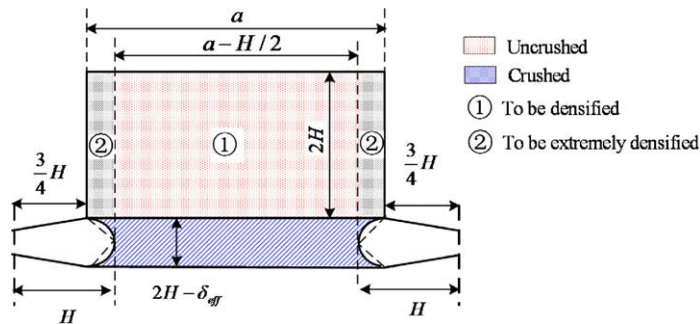$$\Delta V_2 = \frac{1}{8}H(\delta_{eff} + 2H)(4a - H) \tag{42}$$

Fig. 20. Simplified equivalent model for the foam filler.

$$\varepsilon_{f2} = \frac{\Delta V_2}{V_{02}} = \frac{\delta_{\text{eff}} + 2H}{4H} = \frac{1 + \kappa}{2} \tag{43}$$

While κ is among 0.68–0.71, ε_{f1} and ε_{f2} is around 0.68–0.71 and 0.84–0.86, respectively. Substituting $\varepsilon_c = 0.55$, $\varepsilon_{f1} = 0.70$ and $\varepsilon_{f2} = 0.85$ into Eq. (29), the mean stresses of densified region and extremely densified region are

$$\bar{\sigma}(\varepsilon_{f1}) = 1.1016\sigma_p$$
$$\bar{\sigma}(\varepsilon_{f2}) = 1.9930\sigma_p \tag{44}$$

respectively. It shows that although the strain is only 0.15 higher, the mean stress of extremely densified region is 1.8 times as much as that of densified region in this model. Similarly, the energy absorption of foam-filler is

$$E_{\text{foam}} = \sigma_p[C_1(2a - H)^2 + C_2 H(4a - H)] \cdot 2H \tag{45}$$

where coefficients $C_1 = 0.1928$ and $C_2 = 0.4235$. The mean crushing force of foam-filled top-hat is

$$\overline{P}_{\text{s,filled}} = \left\{ M_0\left(A_1\frac{r}{t} + A_2\frac{L}{H} + A_3\frac{H}{r}\right) + \sigma_p[C_1(2a - H)^2 + C_2 H(4a - H)] \right\}\frac{2H}{\delta_{\text{eff}}} \tag{46}$$

And the minimum condition leads to

$$2\sigma_p(C_2 - C_1)H^3 - 4\sigma_p a(C_2 - C_1)H^2 - M_0\sqrt{\frac{A_1 A_3 H^3}{t}} + M_0 A_2 L = 0 \tag{47}$$

Eq. (47) is in the similar form as Eq. (37).

The simplified model gives an even better prediction, and the predicted mean crushing forces are amazingly accorded to those of experimental, with an error of 5.3% for the top-hat and 1.6% for the double-hat, respectively. Table 6, containing the similar information as that of Table 5, gives the energy absorption partition and contribution of each component to the interaction effect by the simplified model.

These two models give the same tendency while evaluating the relative interaction effect of each component, despite some variations in the representative model. This indicates, when an appropriate relationship between the wavelength of the metal column and the volume change of the foam filler is built, reasonable solutions could be reached.

Diagrams containing the similar information as those in Fig. 16–19 can be plotted based on Eq. (47). Here only the diagram showing contributions of densified region and extremely densified region is listed, see Fig. 21. The contribution of extremely densified region seems to be lower than that of the previous model, due to a smaller volumetric fraction in the simplified model.

5.2. The mechanism of interaction effect

Both numerical simulation and analytical model give the conclusion that aluminum foam filler contributes predominantly to the interaction effect. When filled into the hat section, both volume reduction ΔV and

Table 6
Partition energy absorption and contribution of interaction effect via the simplified model, in term of mean crushing force P_m

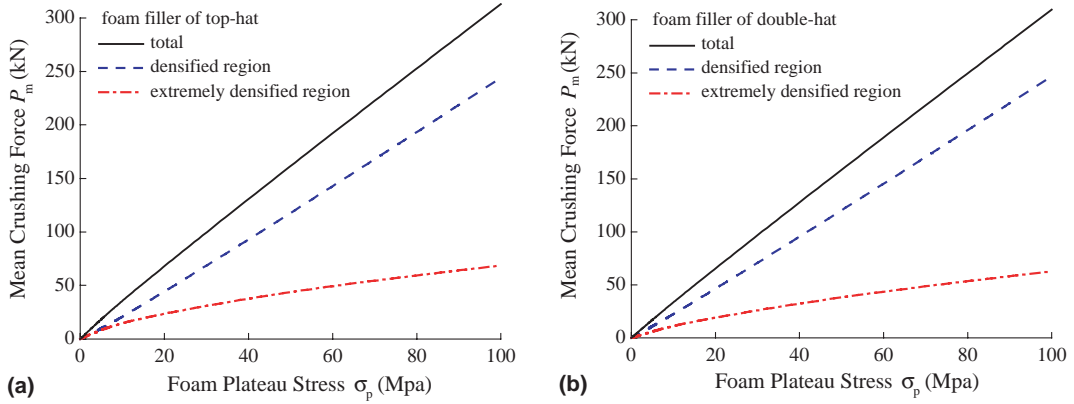| Type	Individuals			Foam-filled components			Contribution to the interaction effect		
	Empty hat (kN)	Free foam column (kN)	Sum (kN)	Hat section component (kN)	Foam filler component (kN)	Total (kN)	Increase in hat section kN/(%)	Increase in foam filler kN/(%)	Total increase kN/(%)
Top-hat	40.8	12.24	52.32	42.92	17.75	60.67	2.12/(5.2)	5.51/(45.0)	8.35/(16.0)
Double-hat	64.8	12.24	77.04	67.67	16.45	84.13	2.87/(4.4)	4.21/(34.4)	7.09/(9.2)

Fig. 21. Contributions of densified region and extremely densified region to the energy absorption, respectively: (a) foam-filled top-hat; (b) foam-filled double-hat.

mean stress $\bar{\sigma}$ of the foam filler increased, due to the elevated final strain ε_f. As a result, energy absorption in the foam is greatly increased, according to Eq. (19). The local strain may exceed 0.8, which is in a sharp contrast to the 0.6 strain of the unbounded foam column when uniaxially crushed. According to the analytical model, while compared with the free foam column, the mean crushing force of the foam filler may increase by 46.5% and 37.6%, for the filled top-hat and double-hat, respectively.

In contrast, the hat section component increase only by 5.8% and 4.6% for the filled top-hat and double-hat, respectively. Referring to Table 4, the half wavelength H decreases from 18.3 mm to 14.5 mm for the filled top-hat, and from 11.5 mm to 10.3 mm for the filled double-hat. Fig. 17 reveals that the shortening in H accounts for only 1.4% and 0.4% increase in the mean crushing force, for the top-hat and double-hat, respectively. Therefore, the main reason accounts for the interaction effect from the hat section component is the decreased effective crushing force δ_{eff}.

5.3. Including effect of aluminum foam density

Eq. (28) does not contain foam density information. Previous studies show that foam density is one of the key factors that affect the crushing behavior of the aluminum foam and the filled structures. Gibson and Ashby (1997), Hanssen et al. (2000c) and Reyes et al. (2004) found that aluminum foams obey the power-law relationship

$$\sigma_p = C_{pow} \left(\frac{\rho_f}{\rho_{f0}} \right)^m \tag{48}$$

where C_{pow} and m are material constants, ρ_{f0} is the density of the foam base material, which is 2.7 g/cm³ for aluminum.

The crushing behavior of the foam material is seriously dependent upon manufacturing method and foam type. We (Song and Fan, 2004) examined the crushing behavior of aluminum foam manufactured from melt route technique with foam density of $\rho_1 = 0.20, 0.25, 0.37$ and 0.40 g/cm³, and found a linear relationship between the plateau stress and foam density

$$\sigma_p = 0.99 + 15.59\rho_f \tag{49}$$

Suppose the crushing history after densification strain ε_c could be fitted with the exponential function in the same form of $F(x)$ in Eq. (28), substitute σ_p with $f(\rho_f)$ in Eq. (28), where $f(\rho_f)$ can be in the form of Eq. (48)

or Eq. (49), the current model could be generalized. Again, this is under the assumption that volumetric reduction is not seriously affect by the foam density (or plateau stress).

6. Conclusions

Numerical simulation and analytical model give the similar tendency while partitioning energy absorption and determining the contribution of interaction effect in the foam-filled hat sections. When a hat-section is filled with aluminum foam, increase in energy absorption was found both in hat section component and foam-filler component, whereas the latter contributes predominantly to the interaction effect.

In the numerical simulation, the contribution to the interaction effect resulted from the hat section component is 4.27 kN (or 10.4% increase) and 2.68 kN (or 4.1% increase) for filled top-hat and double-hat, respectively, and the contribution to the interaction effect resulted from the foam filler component is 5.13 kN (or 58.1% increase) and 3.71 kN (or 42.1% increase) for filled top-hat and double-hat, respectively, and the overall interaction effect is 9.40 kN (or 18.9% increase) and 6.39 kN (or 8.5% increase) for filled top-hat and double-hat, respectively. Comparably, in the analytical model, the contribution to the interaction effect from the hat section component is 2.35 kN (or 5.8% increase) and 2.96 kN (or 4.6% increase), the contribution to the interaction effect from the foam filler component is 5.69 kN (or 46.5% increase) and 4.60 kN (or 37.6% increase), and the overall interaction effect is 8.76 kN (or 16.7% increase) and 7.56 kN (or 9.8% increase), for filled top-hat and double-hat, respectively. It seems that the interaction effect in the filled top-hat section is slightly more obvious.

The results from analytical models seem to be more reliable, and the total error is within 6% when compared with the experiment. The results from the numerical simulation, however, give a qualitative rather than a quantitative evaluation, because the dynamic effect cannot completely eliminated from the model.

The extremely densified region in the crushed foam filler accounts for further the interaction effect. To model the energy absorption behavior of the foam-filled structure successfully, one fundamental work is properly determining the volume reduction ΔV and the mean stress $\bar{\sigma}$ at a specific strain ε_f. Therefore, reasonable volume relationship and the constitutive relationship of the foam need to be carefully built.

This analytical work is instructive to understand the energy absorption mechanism of foam-filled structures, and further investigation may be carried out in the experimental category to examine some details and also predictions of current work.

References

Abramowicz, W., Wierzbicki, T., 1988. Axial crushing of foam-filled columns. International Journal of Mechanical Sciences 30 (3/4), 263–271.

Abramowicz, W., Wierzbicki, T., 1989. Axial crushing of multicorner sheet metal columns. Journal of Applied Mechanics 56 (3), 113–120.

Chen, W.G., 2001. Experimental and numerical study on bending collapse of aluminum foam-filled hat profiles. International Journal of Solids and Structures 38 (44–45), 7919–7944.

Gibson, L., Ashby, M., 1997. Cellular Solids. Structure and Properties. Cambridge University Press, Cambridge.

Hallquist, J.O., 1998. Theoretical Manual. Livermore Software Technology Corporation, California.

Hanssen, A.G., Langseth, M., Hopperstad, O.S., 1999. Static crushing of square aluminium extrusions with aluminium foam filler. International Journal of Mechanical Sciences 41 (8), 967–993.

Hanssen, A.G., Langseth, M., Hopperstad, O.S., 2000a. Static and dynamic crushing of circular aluminium extrusions with aluminium foam filler. International Journal of Impact Engineering 24 (5), 475–507.

Hanssen, A.G., Hopperstad, O.S., Langseth, M., 2000b. Bending of square aluminium extrusions with aluminium foam filler. Acta Mechanica 142 (1–4), 13–31.

Hanssen, A.G., Langseth, M., Hopperstad, O.S., 2000c. Static and dynamic crushing of square aluminium extrusions with aluminium foam filler. International Journal of Impact Engineering 24 (4), 347–383.

Hanssen, A.G., Hopperstad, O.S., Langseth, M., 2001a. Design of aluminium foam-filled crash boxes of square and circular cross-sections. International Journal of Crashworthiness 6 (2), 177–188.

Hanssen, A.G., Langseth, M., Hopperstad, O.S., 2001b. Optimum design for energy absorption of square aluminium columns with aluminium foam filler. International Journal of Mechanical Sciences 43 (1), 153–176.

Hanssen, A.G., Hopperstad, O.S., Langseth, M., 2002. Validation of constitutive models applicable to aluminum foams. International Journal of Mechanical Sciences 44, 359–406.

Kim, H.S., Chen, W., Wierzbicki, T., 2002. Weight and crash optimization of foam-filled three-dimensional "S" frame. Computational Mechanics 28 (5), 417–424.

Reddy, T., Wall, R., 1988. Axial compression of foam-filled thin-walled circular tubes. International Journal of Impact Engineering 7, 151–166.

Reyes, A., Hpperstad, O., Langseth, M., 2004. Aluminum foam-filled extrusions subjected to oblique loading:experimental and numerical study. International Journal of Solids and Structures 41, 1645–1675.

Santosa, S., Wierzbicki, T., 1998. Crash behavior of box columns filled with aluminum honeycomb or foam. Computers & Structures 68 (4), 343–367.

Santosa, S., Wierzbicki, T., 1999. Effect of an ultralight metal filler on the bending collapse behavior of thin-walled prismatic columns. International Journal of Mechanical Sciences 41 (8), 995–1019.

Santosa, S., Wierzbicki, T., Hanssen, A.G., Langseth, M., 2000. Experimental and numerical studies of foam-filled sections. International Journal of Impact Engineering 24 (5), 509–534.

Seitzberger, M., Rammerstorfer, F.G., Gradinger, R., Degischer, H.P., Degischer, H.P., Walch, C., 2000. Experimental studies on the quasi-static axial crushing of steel columns filled with aluminium foam. International Journal of Solids and Structures 37 (30), 4125–4147.

Song, H.W., Fan, Z.J., 2004. Energy absorption behavior of aluminum foam-filled hat sections. Postdoctoral Report, Tsinghua University, Beijing.

White, M.D., Jones, N., 1999a. Experimental quasi-static axial crushing of top-hat and double-hat thin-walled sections. International Journal of Mechanical Sciences 41 (2), 179–208.

White, M.D., Jones, N., 1999b. A theoretical analysis for the dynamic axial crushing of top-hat and double-hat thin-walled sections. Proceedings of the Institution of Mechanical Engineers Part D—Journal of Automobile Engineering 213 (D4), 307–325.

Wierzbicki, T., Abramowicz, W., 1983. On the crushing mechanics of thin-walled structures. Journal of Applied Mechanics 50 (12), 727–733.